

# Ultra-Efficient On-Device Object Detection on AI-Integrated Smart Glasses with TinyissimoYOLO

Julian Moosmann<sup>\*†</sup>, Pietro Bonazzi<sup>\*†</sup>, Yawei Li<sup>†</sup>, Sizhen Bian<sup>†</sup>, Philipp Mayer<sup>†</sup>, Luca Benini<sup>†‡</sup>, Michele Magno<sup>†</sup>

<sup>†</sup>Dept. of Information Technology and Electrical Engineering, ETH Zürich, Switzerland

<sup>‡</sup>Dept. of Electrical, Electronic and Information Engineering, University of Bologna, Italy

**Abstract**—Smart glasses are rapidly gaining advanced functionality thanks to cutting-edge computing technologies, accelerated hardware architectures, and tiny Artificial Intelligence (AI) algorithms. Integrating AI into smart glasses featuring a small form factor and limited battery capacity is still challenging when targeting full-day usage for a satisfactory user experience. This paper illustrates the design and implementation of tiny machine-learning algorithms exploiting novel low-power processors to enable prolonged continuous operation in smart glasses. We explore the energy- and latency-efficient of smart glasses in the case of real-time object detection. To this goal, we designed a smart glasses prototype as a research platform featuring two microcontrollers, including a novel milliwatt-power RISC-V parallel processor with a hardware accelerator for visual AI, and a Bluetooth low-power module for communication. The smart glasses integrate power cycling mechanisms, including image and audio sensing interfaces. Furthermore, we developed a family of novel tiny deep-learning models based on YOLO with sub-million parameters customized for microcontroller-based inference dubbed TinyissimoYOLO v1.3, v5, and v8, aiming at benchmarking object detection with smart glasses for energy and latency. Evaluations on the prototype of the smart glasses demonstrate TinyissimoYOLO’s 17ms inference latency and 1.59mJ energy consumption per inference while ensuring acceptable detection accuracy. Further evaluation reveals an end-to-end latency from image capturing to the algorithm’s prediction of 56ms or equivalently 18 frames per seconds (FPS), with a total power consumption of 62.9mW, equivalent to a 9.3 hours of continuous run time on a 154mAh battery. These results outperform MCUNet (TinyNAS+TinyEngine), which runs a simpler task (image classification) at just 7.3 FPS per second.

**Index Terms**—AIoT, edge processing, image processing, neural networks, object detection, smart glasses, system design, TinyML, YOLO

## I. INTRODUCTION

The rapid integration of cutting-edge technologies of perception and computing into wearable devices has ushered in a transformative era, redefining how we engage with our surroundings and environment [1], [2]. Among innovative wearables, smart glasses stand out as the next big market for wearable computing [3]. Their multifaceted applications span across a diverse spectrum of fields, offering valuable support to skilled professionals [4], while at the same time elevating user experiences in entertainment and education [5], and most importantly, enhancing the quality of life for individuals with disabilities [6], [7].

\* These authors contributed equally.



Figure 1. **Smart Glasses with Electronics**: The designed smart glasses hardware. The left hanger holds the miniaturized electronics. The right hanger contains the battery, with an energy content of up to 154mAh.

The ever-expanding mass adoption and widespread system deployment of current AI technology are accentuating the trend toward edge intelligence [8], [9], targeting computer vision [8], [10], biomedical applications [11], [12], natural language processing [13], and many other spaces [2]. In particular, in the domain of computer vision, deep learning approaches have revolutionized semantic scenery understanding [8], [14]. Understanding the environmental context in which smart devices operate, whether they are autonomous robots, Artificial Intelligence of Things (AIoT) devices, environmental or health monitoring tools, plays a pivotal role in the detection and localization of objects [15], [16], environmental mapping [17], [18], and facilitating navigation [19] in human-centric surroundings. Embedding machine learning into glasses not only enhances the AIoT device capabilities but also brings intelligence right to the user’s fingertips, or perhaps more fittingly, to their forehead. This goal poses the challenge of compressing and running Artificial Intelligence (AI) algorithm inference directly on the low-power edge processors.

On the other hand, state-of-the-art (SOTA) image processing algorithms are predominantly designed for best accuracy performance and thus typically entail execution in the cloud [20] or power-hungry embedded systems on chip, such as those available on mobile phones. All the hardware platforms vastly exceed the power constrain of small-size smart glasses batteries. Today, SOTA algorithms often have network sizes in the order of hundreds of megabytes to a few gigabytes, rendering them unsuitable for execution on edge microcontrollers with at most a few megabytes of memory [21]. For instance, the You Only Look Once (YOLO) [22] algorithm, is an optimized

deep learning algorithm with a memory requirement of a few hundred megabytes and is used to perform real-time object detection on GPU-class devices [23].

Commercially available smart glasses such as the newly released RayBan Meta, Vuzix® smart glasses family, make use of Qualcomm’s Snapdragon AR1/XR1 processor with a power budget of few hundreds of milliwatts. Despite the choice of using high-performance processors, the on-board computer is used for transmitting the vast amount of data taken with high-resolution cameras and microphones, while image or speech processing is minimally done on-device, making the ‘smart’ glasses only a datalogger. Bringing the processing on-device with low-power processors has the advantage of drastically increasing user privacy while decreasing inference latency and possibly power consumption, as it avoids transmitting a high volume of data to the cloud [24].

To bridge the gap between the available computational resources and the demands of AI algorithms, there has been a growing trend in recent years towards the development of novel processing units. These units are armed with innovative energy-efficient cores, such as RISC-V cluster cores for parallel processing of workloads, as well as dedicated accelerated hardware with specialized co-processors [25]–[27]. Therefore, while new hardware is being developed new small-sized and efficient, lightweight, and quantized networks are being proposed to achieve near SOTA algorithm accuracy while having small-sized memory footprints [10], [28]. Combining those novel multi-core RISC-V processors, with a dedicated system design for ultra-low power consumption, and designing tiny and lightweight optimized AI algorithms enable smart glasses system achieving long-lasting battery run-time.

This paper presents the design and implementation of an energy-efficient intelligent smart glasses system—see Fig. 1—equipped with a novel RISC-V-based System-on-Chip (SoC) called GAP9 from Greenwaves Technologies. GAP9 also includes a power-efficient Machine Learning (ML) accelerator where the proposed lightweight and quantized YOLO-based algorithms are evaluated. Our contributions can be summarized as follows:

- 1) **Smart Glasses’ System Architecture:** We propose a novel system architecture tailored for smart glasses applications, integrating a power-efficient ML accelerator. This architecture optimally balances processing power and energy consumption, enabling real-time on-device inference of deep neural networks for various machine learning tasks.
- 2) **Sub-Million Parameter YOLO Architectures:** We design and present a series of custom YOLO architectures engineered to operate within the constraints of sub-million parameters. We reduced the memory footprint and computational requirements, making the newest version of YOLO algorithms amenable for deployment on resource-constrained devices without significant accuracy loss.
- 3) **Real-world Deployment:** We demonstrate the practical applicability of our proposed system by deploying

the optimized YOLO architectures on the smart glasses platform and by predicting images from the real world. The deployment ensures the efficacy of our approach in enabling real-time, on-device inference for a wide array of computer vision tasks, ranging from object detection to, in the future, actual scene understanding.

- 4) **Power Efficiency and Performance Evaluation:** We conduct extensive experiments to validate the power efficiency and performance of our smart glasses system. Comparative analyses against commercial edge vision systems reveal superior energy efficiency and longer battery life for our system.
- 5) **Open-Source Implementation:** To facilitate reproducibility and encourage further research, we release the source code of our optimized TinyissimoYOLO architecture versions, allowing the community to build upon our work and extend it to new application domains.

The paper is structured as follows: in Section II, we investigate recent related works from the literature regarding both the SOTA object detection neural networks and their deployability onto microcontrollers using different frameworks. Section III introduces the prototype design of the smart glasses aiming for latency and energy efficiency during on-board AI execution. The TinyissimoYOLO networks are described in Section IV. The evaluation metrics and results are given in Section V and Section VI, including the detection results and the system evaluation of GAP9 integrated in the proposed smart glasses. Finally, we summarize our work in Section VII and Section VIII with a discussion of current limitations and future work.

## II. RELATED WORK

In the following section, an overview of state-of-the-art object detection algorithms is provided while further discussing the state-of-the-art for object detection on microcontrollers. An in-depth discussion is provided about the trilemma between network accuracy, computational capacity, and development difficulty to deploy networks on such tiny edge devices. Last but not least, currently available smart glasses on the market as well as research projects are summarized and set into perspective while this work is further motivated.

### A. SOTA Object Detection

YOLO [22], is an optimized deep learning algorithm used to perform real-time object detection on GPU-class devices [23]. It utilizes a feature extraction Convolutional Neural Networks (CNN) backbone and detection head to perform localization of the extracted semantic information. Meanwhile, there exist a family of different YOLO versions which utilize all the same backbone, and head structure while only differing in network size, inter-network connection, and used layer operations [29]–[35]. In contrast to R-CNNs [36]–[38] or SSDs [39], [40], the YOLO networks are all single-shot detection networks. Nevertheless, the majority of object-detection networks require power-hungry GPUs for inference execution and are as such unsuitable for deployment on edge devices [14], [41], [42].

New detection networks are based on vision transformers [43], [44] exaggerated due to the popularity of the latest large language models [13]. Powerful edge computing platforms, such as NVIDIA Tegra can run SOTA detection networks at high frame rates with a power budget of several tens of watts [21], [45], [46]. Further, the memory requirement to run such inferences are of megabytes for running at sensor rate [47], [48].

In this work, despite previous works that focus on performance in power-hungry processors, our primary focus lies in the design and deployment of all major YOLO versions, while also exploring the trade-offs associated with various quantized and compressed versions of YOLO targeting deployment on milliwatt-class processors. This research addresses the critical need for efficient, low-power object detection solutions, contributing to the development of cutting-edge applications in resource-constrained edge computing environments. To address the portability of SOTA object detection algorithms onto milliwatt microcontroller devices, several techniques are exploited to enable milliwatt power and real-time object-detection inference execution on Internet of Things (IoT) or AIoT devices [47], [49].

### B. SOTA on MCU

TinyissimoYOLO [28] and its successor [50] try to bridge the gap between accuracy and network size [21], while maximizing the available compute acceleration on the milliwatt edge device. TinyTracker [10] exploits the full acceleration capabilities by implementing AI "in-sensor" achieving a 19ms end-to-end total latency and 5mJ end-to-end total energy in IMX500, 34.4ms&34.2mJ on Coral Micro, and 234mJ&522ms on Spresense, separately. Researchers also proposed new algorithms for specialized use-cases [51], [52] or for specialized on-board sensor processing [53]. Some techniques exploit the idea of neural architecture search, for automatically creating the best network given a constrained search space [54], [55]. Other techniques quantize the network weights to the extreme [56]–[59] or using quantization-aware training and apply techniques such as pruning [47], [60]. These techniques are used to minimize the network's size and as such memory consumption, while maintaining or only marginally decreasing the accuracy of the original network.

As has been shown by the TinyissimoYOLO networks [28], [50], where a comparison was carried out between several ARM-Cortex M4 and M7 microcontrollers from STMicroelectronics, and from Ambiq (an ultra low-power MCU using sub-threshold technology), the MAX78000 microcontroller from Analog Devices, which exploits a state-of-the-art hardware accelerator for CNN networks, and a RISC-V low power parallel processors with hardware accelerator, GAP9 from Greenwaves Technologies. This work showed that MAX78000 is parallelizing the compute workload best. Although GAP9 achieves the same energy efficiency even though having two-fold less MAC/cycle, MAX78000 has a highly optimized but inflexible hardware accelerator, which is not allowing networks to be larger than 442 kB while only supporting a few CNN

layer operations. In contrast, the GAP9 has a neural engine that can access internal and external memory—as such is not bound to on-chip memory storage—and has no strict layer operation restrictions.

Therefore, this paper leverages the GAP9's exceptional energy-efficient parallel processing capabilities and integrates it with low-power Bluetooth Low Energy (BLE) transceiver chip. This combination forms the backbone of our design to facilitate robust object detection in smart glasses with seamless connectivity.

### C. Custom Silicon

Trying to bridge the worlds from a more hardware-specific side, Application Specific Integrated Circuits (ASICs) or Field-Programmable Gate Arrays (FPGAs) implementations are trying to overcome Central Processing Unit (CPU) limitations, by dedicating specific parts of silicon to the sole purpose of executing AI algorithms [27]. The Marsellus SoC, is a fully open source RISC-V based AIoT end-node making use of the open source Intellectual Property (IP)—the Reconfigurable Binary Engine (RBE) [25]—, which can accelerate 3x3 and 1x1 convolutions (incl. pointwise convolutions) with reconfigurable data-paths for 2-8bit activation and 2-8bit weight, enabling full support for Quantized Neural Networks (QNNs). Another such example is the ITA accelerator [26], which is another open-source IP, targeting attention and softmax acceleration for quantized transformers. Deep Learning Accelerator Unit (DLAU), is an FPGA-based architecture, which illustrates the user-defined trade-off between energy consumption and computing speed. In-sensor and near-sensor data-processing [61], [62] is a possible solution to further decrease latency and energy, on the cost of losing general compute capability. Such sensors have built-in processing units, as for example the commercially available IIS2ICLX from STMicroelectronics with its decision-tree-like embedded machine-learning core. Another example is Sony's IMX500 image sensor which is fused with an AI engine to perform inference of QNNs on the sensor itself. Research projects utilize the same idea, for in-sensor data processing while deploying a High Dimensional (HD) computing classifier onto an FPGA to perform hand-gesture recognition [12]. The recent works on custom silicon show that our design exploiting the utilization of the GAP9 microcontroller, in conjunction with low-power BLE technology, aligns with the prevailing trend of pushing computation closer to sensors and deploying efficient, specialized hardware to bridge the gap between AI algorithms and energy-efficient edge computing.

### D. Deployment Frameworks

To overcome the gap between high-performance and fast GPU-based training and complex deploying of quantized deep learning networks for edge devices—ideally milliwatt low-power microcontroller devices—several specialized deep learning frameworks, targeting simple microcontroller

deployment are created. TensorFlowLite [63], Caffe2Go<sup>1</sup>, CMSIS-NN [64], ARM NN SDK<sup>2</sup>, Greenwaves Technologies' NNTOOL<sup>3</sup>, or Analog Devices AI - Framework<sup>4</sup> are such toolchains. For example, the deployment using TensorFlowLite requires the user to generate a quantized version of its network and export it to a given format. For the quantized version, the tool automatically generates a sample C-code project to be included in the user's application. Analog Devices AI on the other hand is designed for programming their in-house developed accelerator and requires the user to train using PyTorch and custom implementations of their supported functions. Having so, the network can be quantized and exported. The user is further required to describe how the accelerator is able to execute the exported network, such that all 64 processors know where to load and store intermediate data. All of this comes with a certain engineering overhead making it unattractive for rapid development. Nevertheless, these tools are getting improved drastically, and as such, the NNTOOL by Greenwaves Technologies uses an unquantized .onnx file format, which it applies Post-Training Quantization (PTQ) automatically before generating the optimized C-code ready to deploy for its neural engine. In this paper, we present our novel approach to addressing the challenges of high-performance GPU-based models on low-power microcontrollers. Specifically, we focus on the design of different YOLO-based models fully deployable in milliwatt processors. Our work contributes to the ongoing trend of pushing computation closer to sensors and deploying specialized hardware for energy-efficient edge computing, showcasing the potential for efficient object detection in resource-constrained environments.

### E. Smart Glasses

Smart glasses or in-general Augmented Reality (AR) focus on a general computing concept [65] to process the user-device interaction while communicating with cloud or smart-phones via Bluetooth and Wi-Fi [66]. Big tech companies such as Google<sup>5</sup> or Apple<sup>6</sup>, further rely on community APPs being developed and processed on the device, requiring the manufacturer to provide an easy-to-develop software stack, to abstract the hardware from the software. This requires an OS environment to run at reasonably fast speeds, such that user interactions are ensured to run smoothly. In particular, these requirements hinder smart on-device sensor data processing, resulting in the data being processed in the cloud, while data and user privacy are not absolutely contained and guaranteed.

In contrast, several research smart glasses projects aim at the counterpart by running AI algorithms on the device [3], [67]. Others investigate the human-machine interaction with smart glasses [68]. However, many publications focus on a

single smart glasses application scenario and design the system accordingly, e.g., for visually impaired people [6], [7] or smart gadget aid for medical [69], [70] or construction work [71]. Nonetheless, to the best of our knowledge, none of the proposed research prototypes are integratable into the thin frames of the passive glasses [51] and will therefore not be non-stigmatizing nor fashionable, in contrast to actual smart glasses products such as the RayBan-Stories<sup>7</sup> or the brand-new RayBan-Meta<sup>8</sup>. In contrast to many research smart glasses projects, which often lack integration into actual frames, our work introduces a functional and fashionable smart glasses solution with a peak power consumption below 100mW. Our smart glasses are not only aesthetically appealing but also capable of directly executing demanding YOLO object detection tasks, showcasing both efficiency and effectiveness in image processing for real-world applications.

## III. SYSTEM DESIGN

The main goal of this work is to achieve truly smart and energy-efficient glasses. We propose a hardware-software smart glasses solution, eventually eliminating the transmission of private data, and decreasing inference latency while effectively increasing battery run-time.

1) *Smart Glasses Design*: A modular design was targeted so that reuse of the same platform can be guaranteed for other ultra-low power all-day battery runtime AIoT applications. All components are tightly integrated onto a custom, miniaturized Printed Circuit Board (PCB), which can fit inside the plastic housing of glasses and even replace existing PCB of commercial smart glasses.

The design features dedicated low-power infrastructure to power cycle energy-hungry sensors while powering always the minimal required components. This platform is co-designed with a development platform for the rapid integration of further research sensors.

Fig. 2a) shows the hardware overview. The development board is shown on the left, while the smart glasses electronics is the zoomed-in PCB (green) on the development board. The right side of the Fig. 2b) describes the hardware using a block-diagram. The left side shows the development board, while the zoomed-in version is the smart glasses electronics. The M2 connector aims for development and reusability. To further minimize the form factor and fit temples of smart glasses, several on-board sensors are left away, resulting in the design that can be seen in Fig. 3. The final miniaturized smart glasses PCB fits smoothly inside the temple of glasses, see Fig. 1.

*Smart Glasses electronics*: The platform can be broken down to the following three main parts:

- Battery and power management
- Dual-microcontrollers energy-efficient architecture
- Various sensors, e.g. IMU, multiple cameras, and micro-phones.

<sup>1</sup><https://engineering.fb.com/2016/11/08/android/delivering-real-time-ai-in-the-palm-of-your-hand>

<sup>2</sup><https://github.com/ARM-software/armnn>

<sup>3</sup>[https://github.com/GreenWaves-Technologies/gap\\_sdk](https://github.com/GreenWaves-Technologies/gap_sdk)

<sup>4</sup><https://github.com/MaximIntegratedAI>

<sup>5</sup><https://developers.google.com/glass-enterprise/>

<sup>6</sup><https://developer.apple.com/visionos/>

<sup>7</sup><https://tech.facebook.com/2023/2/the-making-of-ray-ban-stories/>

<sup>8</sup><https://about.fb.com/news/2023/09/new-ray-ban-meta-smart-glasses/>

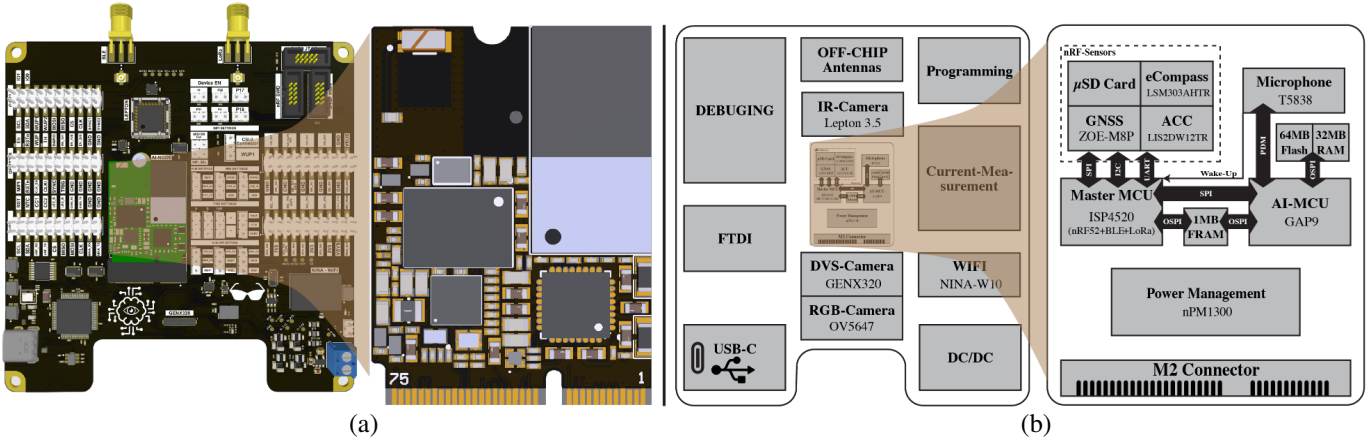


Figure 2. **Development Board:** a) The proposed hardware system consists of two boards. The board on the left—development board—is shown, featuring additional power circuitry, multiple camera interfaces, Wi-Fi, and debug possibility. The smart glasses board—zoomed in—, features two microcontrollers, several sensors, and a power management system for stand-alone operation. b) shows the hardware block diagram for the development and smart glasses board respectively.

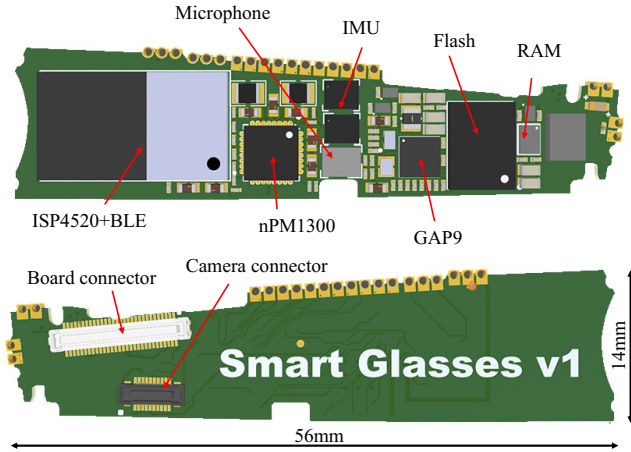


Figure 3. **Miniaturized Smart Glasses Electronics:** The designed smart glasses hardware, which fits inside actual frames of glasses.

The battery and power management is needed such that the smart glasses’ electronics can operate untethered. One ultra-low power microcontroller is in charge of wireless communication, low-power signal processing (i.e. data from MEMS sensors), and power management of the various power domains by using multiple power switches in series and parallel within the same voltage levels. To accomplish those tasks the SoC—ISM4520—has been chosen, which features a low-power nRF52 from Nordic Semiconductors microcontroller with a built-in ARM Cortex-M4 processor, including on-chip BLE. The nRF52 microcontroller inside ISM4520 is not only used to interface the SoC on-chip BLE. In addition, a more power and energy-efficient RISC-V parallel processor, GAP9 from Greenwaves Technologies, is used for enabling computational intensive on-the-edge AI algorithm inference for image and audio processing using neural networks. GAP9 enables both parallelization and hardware acceleration while the GAP9 achieves the overall best trade-off performance in

few milliwatts envelope, considering latency, energy consumption per inference, and parallelization of the computation. In particular, the GAP9 SoC has a built-in general-purpose neural network accelerator capable of running SOTA algorithms’ operations whenever the algorithm fits inside the memory. An FRAM is placed such that both GAP9 and nRF52 can access a shared memory-space to share sensor data and system states. Additionally, GAP9 has a big amount of off-chip memory such as 64 MB of Flash and 32 MB DRAM. Since cameras will be directly interfaced with GAP9—via connectors on the development board—the GAP9, memory is needed for buffering the sheer amount of data.

The M2 PCB smart glasses electronics features additional sensors, such as the eCompass—LSM303—, the Accelerometer—LIS2DW—, GNSS module—ZOE-M8B—, Microphones with wake-up capabilities—T5838—and an on-board micro-SD card storage for gigabytes of data collection. Removing the GNSS module of the M2 PCB allows all the electronics design to be shrunk into a trapezoidal form factor, Fig. 3 of 14 mm x 36 mm with a height of 3 mm such that the electronics fit inside a temple of a glasses’ frame, see Fig. 1.

*The development board*—see Fig. 2—is designed for modular, rapid design and integration of various new sensors. The main focus is on the design of GAP9’s interfacing with different cameras using the CSI-2 protocol. The single-line CSI-2 interface is multiplexed to interface two cameras. Once a connector for interfacing commercial of the shelf (COTS) RGB cameras, designed for use with Raspberry Pis has been added. This interface is shared with a second camera connector, specifically designed for the new event-based camera GENX320 from Prophesee. As a third camera option, a Lepton3.5 is added to the development board for adding infrared camera capabilities and interfaced via SPI. For debugging purposes, the Wi-Fi chip NINA-W10 with an on-chip antenna is added to possibly stream data. For easy debug and development, specifically for the GAP9, but also for the U-BLOX GNSS and Wi-Fi chip a further quad-channel FTDI

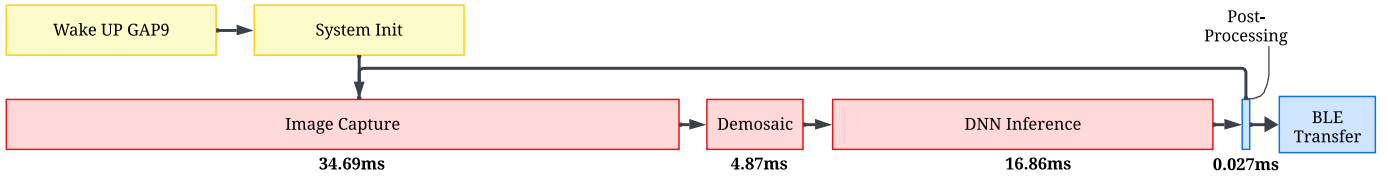


Figure 4. **Demonstrator Firmware Overview:** The image shows the flow chart of the demonstrator firmware, including the execution latency for the corresponding task. The box sizes is in relative size to the execution time.

chip is added, allowing programming of GAP9 seamlessly via USB-C connection to a host laptop.

2) *Demonstrator:* To showcase on-board intelligence and longer battery runtime, a demonstrator firmware has been designed and deployed into the GAP9 hardware. This features image capturing, image debayering, inference of a multi-object detection network, see Section IV-A, and output post-processing of the network inference. Fig. 4 shows the execution pipeline. On purpose, the implementation of the nRF52 firmware is left aside to show non-stop and non-interrupted demonstrator operation. Therefore, sending the information via BLE to a demonstrator APP for visualization purposes is not considered, and its power and energy consumption is not included in the battery runtime estimation. Still, a power estimate is provided, considering the nRF controller is always in sleep mode, wakes up for a very short amount of time to reconfigure power distribution, and goes to sleep mode again. This choice is driven by the fact that the nRF52’s system housekeeping part’s only purpose is to extend the battery run-time. As such, power cycling un-used sensors, power cycling GAP9 when not in use, and further setting the glasses into ultra-low power states. Literature shows [72] that tightly integrating low-power modes into a system’s firmware will lead to a drastic increase of battery runtime. As such, this paper only reports a worst-case always-on demonstrator firmware to showcase the capabilities of the proposed system.

#### IV. NEURAL NETWORK ARCHITECTURES

This section presents a family of sub-million parameter detection algorithms, based on a different version of the YOLO architecture, which we have developed for accelerated micro-controllers or in general low-power edge processors. To have the right trade-off computational resources and performance for smart glasses, multi-object-class probability and bounding box predictions from 256x256 resolution images have been proposed. However, the networks can be adapted for larger and smaller resolutions.

##### A. Model Architecture

YOLOv5, and YOLOv8 employ different backbone and head architectures to predict class probabilities and bounding boxes. We accurately evaluated the respective versions to extract their performance under sub-million parameter constraints, see the network specifications in Table I. This has been conducted to establish a family of networks suitable to be deployed on AIoT devices. In particular, for the deployment of

multi-object detection networks on a microcontroller with ML acceleration, such as the GAP9. All the networks described below have been deployed on the GAP9 and not only will their detection capability be evaluated, but also their deployed inference performance, energy consumption, and their ability to parallelize the inference execution on such a hardware.

TinyissimoYOLO and TinyissimoYOLO-v1.3 represent significant evolutionary steps in object detection architectures. The key differentiator lies in the incorporation of the Detection Block from the V8 architecture into the final prediction layer of TinyissimoYOLOv1.3 and its training with a Multi-Object Detection Loss described in Section IV-C. This strategic enhancement imbues the latter with heightened sensitivity and a larger number of detection parameters. Consequently, TinyissimoYOLOv1.3 demonstrates superior performance in scenarios demanding precise object detection.

TinyissimoYOLO-v5’s architecture features a Cross-Stage Partial (CSP) connection bottleneck module named ‘C3’. In C3, the input is duplicated through two separate 1x1 convolutions which are then concatenated and processed through a final 1x1 convolution to produce the final output. The main distinction between the architecture of YOLOv5 and YOLOv8 lies in the number of convolutions and on the expansion or contraction of the hidden channels in the CSP. Differently from YOLOv5, TinyissimoYOLO-v5 has a layer channel multiple of 0.15 instead of 0.25 (YoloV5-nano) and contains 4 times fewer parameters.

YOLOv8 CSP Block called ‘C2F’, which powers TinyissimoYOLO-v8 starts with a 1x1 convolution that expands the input channels to twice the hidden channel size.

TABLE I  
NETWORK COMPARISON: OF THE NANO YOLO ARCHITECTURES WITH OUR TINYISSIMOYOLO VERSIONS.

| Model             | Layers | Parameters |
|-------------------|--------|------------|
| YOLO-v1-small     | 26     | 45,000k    |
| TY-v1 (Baseline)* | 12     | 422k       |
| TY-v1.3-Small*    | 62     | 403k       |
| TY-v1.3-Big*      | 62     | 959k       |
| YOLO-v5-nano      | 260    | 2,655k     |
| TY-v5-Small*      | 260    | 626k       |
| TY-v5-Big*        | 260    | 889k       |
| YOLO-v8-nano      | 223    | 3,157k     |
| TY-v8-Small*      | 223    | 711k       |
| TY-v8-Big*        | 223    | 839k       |

\* TinyissimoYOLO networks deployed and evaluated on GAP9.

Then, it splits the output into two equal parts and applies a series of bottleneck layers on each part. Finally, it concatenates the processed outputs and applies a second 1x1 convolution. TinyissimoYOLO-v8 has a depth multiple of 0.30 instead of the 0.33 in YoloV8-nano, a layer channel multiple of 0.18 instead of 0.25, and contains 5 times fewer parameters than the nano version.

### B. Input

To improve the training and the robustness for the proposed networks, a series of augmentations is applied to the input 256x256 images of the Pascal VOC dataset [73], to enhance the robustness and diversity of the training data. These augmentations include HSV-Hue with a factor of 0.015, HSV-Saturation with a factor of 0.7, and HSV-Value with a factor of 0.4. Additionally, we apply a 0.1 coefficient to translate the image for both positive and negative directions, and a 0.5 scaling factor for both enlargement and reduction. Furthermore, we perform horizontal flipping with a probability of 0.5 to introduce left-right variations. During training, we also apply the mosaic technique to create composite images for further data augmentation.

### C. Multi-Object Detection Loss

The loss function employed in our model is a weighted combination of three components: box loss ( $\lambda_{\text{box}}$ ), class loss ( $\lambda_{\text{cls}}$ ), and distance-based focal loss ( $\lambda_{\text{dff}}$ ). These components are tuned with specific gain factors to optimize the overall training process:

The box loss term measures the discrepancy between predicted and ground truth bounding box coordinates, with a gain factor of 7.5:

$$\mathcal{L}_{\text{box}} = \lambda_{\text{box}} * \frac{\text{area of overlap}}{\text{area of union}} \quad (1)$$

The class loss, weighted with a gain of 0.5, accounts for the classification error between predicted and actual object classes, and is further scaled with respect to the image resolution:

$$\mathcal{L}_{\text{cls}} = \lambda_{\text{cls}} \times \sum_{i=1}^N \sum_{c \in \text{classes}} (y_{i,c} - p_{i,c})^2 \quad (2)$$

Here,  $y_{i,c}$  is a binary indicator of whether class  $c$  is the correct classification for bounding box  $i$ , and  $p_{i,c}$  is the predicted probability of class  $c$  for bounding box  $i$ .

The distance-based focal loss, with a gain of 1.5, augments the model's sensitivity to hard-to-classify samples, thereby improving classification performance on challenging instances:

$$\mathcal{L}_{\text{dff}} = \lambda_{\text{dff}} \times \sum_{i=1}^N (1 - \text{IoU}_i^{\text{truth}})^\gamma \times (\text{CE}(y_i, p_i)) \quad (3)$$

Here,  $\gamma$  is a hyperparameter controlling the degree of focusing in the focal loss.  $y_i$  is a binary indicator of whether the bounding box is positive or negative, and  $p_i$  is the predicted probability of the bounding box being positive. CE denotes the Cross Entropy Loss.

### D. Training of the Networks

We trained the three models on an NVIDIA GeForce RTX 4090 for 1'000 epochs, with a batch size of 64. The initial learning rate ( $\text{lr}=1\text{e-}3$ ) was reduced using cosine learning rate scheduler to  $1\text{e-}2$  of its value after 3 epoch long warmup phase ( $\text{lr}=1\text{e-}2$ ). We optimize the weights using the SDG algorithm (momentum=0.937) and trained with Automatic Mixed Precision. The networks have been integrated into the Ultralytics framework [34].

Deployment of the networks was done using Greenwaves Technologies' NNTool. Starting of with the unquantized exported .onnx file from the Ultralytics framework, NNTool has an integrated PTQ flow. As such, the networks were deployed using 8-bit integer precision. Once quantized, the network can be auto-tiled by Greenwaves Technologies' Autotiler. This tool is used for automatic code generation, in particular, to generate C-code for the deployment onto the target cores or accelerator (NE16) of GAP9. Further, the user can specify the amount of L1, L2, and L3 memory to be used and the Autotiler tool will generate the network according to the constraints given such that the network is executed with minimal memory wait stalls, depending on each layer's size and operation used. Once the C-code has been generated, the network can be integrated into a custom user-specific project.

## V. EVALUATION METRICS

### A. System Evaluation

The designed system is evaluated by measuring the power consumption and the execution latency of each subprocess of the system demonstrator software.

### B. Hardware Evaluation

Further evaluations were done to assess the network's performance, deployed on the GAP9. This includes inference time, energy efficiency, and assessing the inference efficiency (MAC/cycle) as has been proposed by Giordano et al [74]. All of this is done at a fixed clocking frequency of the SoC GAP9. Additionally, a frequency sweep has been performed to find the Pareto optimal frontier curve for the inference of networks on the NE16 of GAP9 at different frequency and core voltage levels.

### C. Algorithm Evaluation

We consider the mean-average precision (mAP) (mAP50:95) to account for varying confidence thresholds. This metric offers a comprehensive evaluation of detection precision across different object classes.

## VI. RESULTS

### A. System Results

Running the demonstrator on the GAP9, requires the system to wake-up and be powered. Thereafter, initialization of all required processing units of the SoC. Including the NE16 (neural engine, i.e. ML accelerator), initializing the CSI-2 interface for the HM0360 camera from Himax, creating all the needed

memory buffers for image capturing and demosaicing/debayering. Once initialized, the system can go into the demonstration loop, which consists of image capturing, demosaicing of the image, AI inference execution (TinyissimoYOLOv1.3-8) and post-processing of the network output. Fig. 5 shows the power-consumption during full operation of the system, running the loop ten consecutive times. For the following power measurements the loop was executed 100x and the average is reported. Capturing an image 100 times took on average 34.69 ms while consuming 1.17 mJ or 18.79 mA. Demosaicing needed only 4.87 ms while consuming 23.82 mA resulting in 0.209 mJ of energy. Running the small TinyissimoYOLOv1.3 network on NE16 consumed 52.27 mA of current during 16.86 ms resulting in 1.59 mJ of Energy. The rest of the TinyissimoYOLO version is evaluated in Section VI-C. Table II summarizes the current, power, energy measurement for the corresponding demonstration process. Last, the post-processing took 27  $\mu$ s, consuming 28.3 mA resulting in 1.38  $\mu$ J. With that, the average loop execution consumes 3.28 mJ, i.e. 29.55 mA for 61.67 ms.

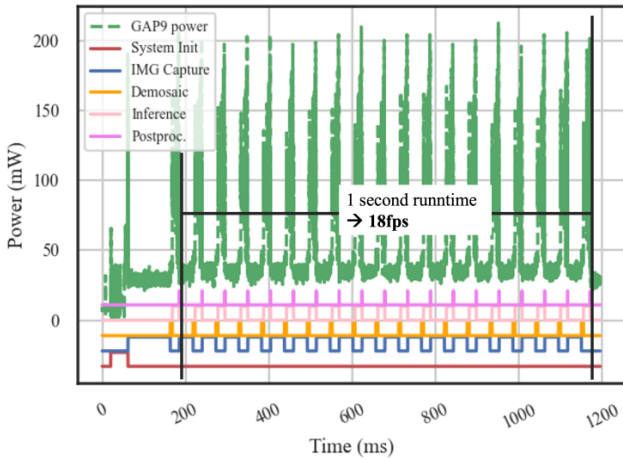


Figure 5. **Full System Power Measurement:** The lines described in the legend show if the mentioned system process is running or not running. We show 18fps GAP9 on-device image-capturing, demosaicing, network inference and postprocessing execution.

TABLE II

SYSTEM DEMONSTRATOR: ENERGY CONSUMPTION MEASUREMENT.

|      | Event                  | Current [mA] | Power [mW] | Energy [mJ] | Time [ms] |
|------|------------------------|--------------|------------|-------------|-----------|
|      | System quiescent*      | 0.75         | 2.48       | 2.48        |           |
|      | Init system            | 11.96        | 21.54      | 0.89        | 41.44     |
| Loop | Capture image          | 18.78        | 33.82      | 1.17        | 34.69     |
|      | Demosaic non-cluster   | 23.82        | 42.88      | 0.21        | 4.87      |
|      | Run Tinyissimoyolov1.3 | 52.27        | 94.10      | 1.59        | 16.86     |
|      | Post processing        | 28.26        | 50.86      | 0.001       | 0.03      |
|      | <b>Loop AVG.</b>       | 30.0         | 54.0       | 3.05        | 56.45     |

\* nRF wakes up from sleep mode, changes power settings, and sleeps again.

## B. Detection Results

In this section, the performance evaluation of the various TinyissimoYOLO network configurations on the PascalVOC test dataset is presented. The results are summarized in Table III and visualized in Table IV using images taken with GAP9—first row of Table IV—, and an Single-Lens Reflex (SLR) camera—second row. The evaluation of TinyissimoYOLO network with different configurations on the PascalVOC dataset reveals a noteworthy improvement in Mean Average Precision (mAP) scores. Specifically, transitioning from TinyissimoYOLOv1.3-Small to TinyissimoYOLOv8-Big architecture results in a substantial mAP enhancement, showcasing the effectiveness of the latter in accurately detecting objects across various classes. The provided visualizations in Fig. 6 illustrate the capabilities of the various TinyissimoYOLO networks compared to the corresponding original YOLO versions of the size nano, illustrating the turn-over point when deployment on GAP9 isn’t possible, at least not for executions with multiple fps.

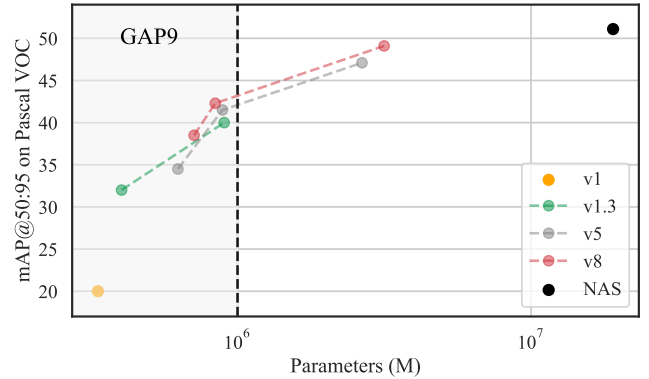


Figure 6. **Parameters Size vs mAP:** TinyissimoYOLOv1.3, v5 and v8 achieves comparable mAP with state-of-the-art YOLO models while running on a microcontroller (GAP9).

## C. Networks Performance on GAP9

The networks were deployed on the NE16 accelerator of GAP9 and compared in terms of latency—Fig. 7a)—, inference efficiency—Fig. 7b)—, and energy per inference—Fig. 7c)—for each TinyissimoYOLO network version v1.3, v5, v8-small/big and NAS. TinyissimoYOLOv1.3 outperforms the other networks in terms of latency with only 16.9 ms execution time. V5 and both v8 variants need 32.7 ms, 34 ms, and 36.6 ms, respectively. In terms of inference efficiency, v1.3 is best parallelizable with up to 43.37 MAC/cycle. The v5 and v8 versions have 16.28 MAC/cycle, 14.98 MAC/cycle, 15.27 MAC/cycle, respectively. Since v1.3 performs fastest and most parallelized, it’s also the most energy efficient with only consuming 1.27 mJ, followed by v5 consuming 2.34 mJ, v8-small with 2.48 mJ and v8-big consuming 2.62 mJ.

Deploying the networks at different clocking frequencies of the NE16 core at different voltage levels leads to a Pareto

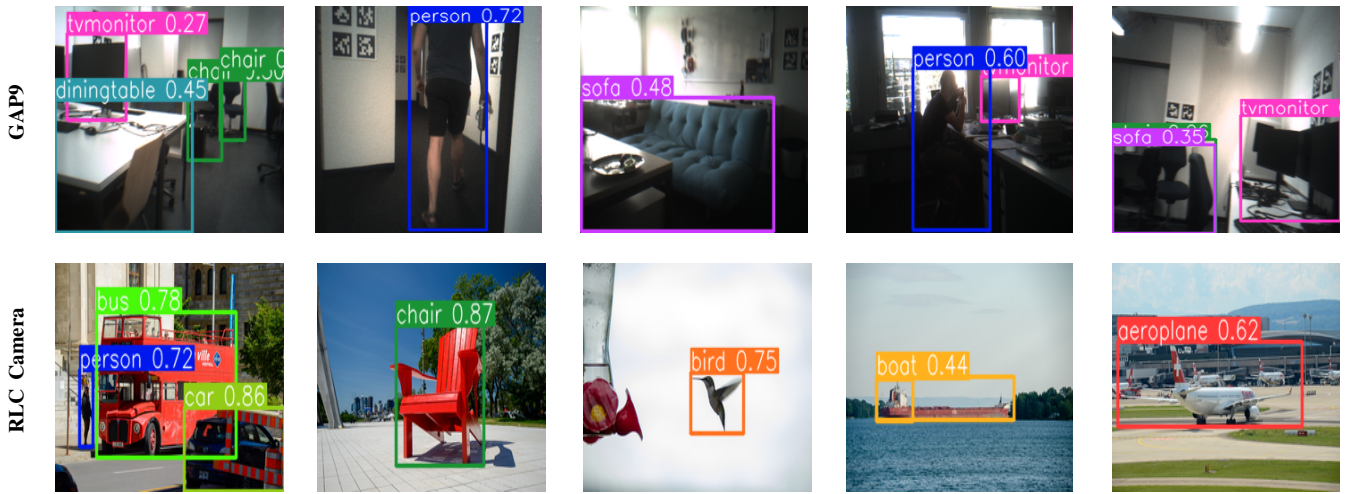
TABLE III

**TINYISSIMOYOLO MAP:** NETWORKS TRAINED AND EVALUATED ON PASCALVOC WITH AN INPUT RESOLUTION OF 256X256 PIXELS. THIS TABLE SHOWS HOW DIFFERENT VERSION OF THE NETWORK PERFORM. THE NAMING CONVENTION OF THE DIFFERENT NETWORK CONFIGURATIONS FOLLOWS THE CODE: TY(TINYISSIMOYOLO)-YOLOVERSION-SIZE, FOR MORE DETAILS SEE: SECTION IV.

| Network         | mAP |      |      |      |      |        |     |     |     |       |     |       |     |       |       |        |       |       |      |       |     |
|-----------------|-----|------|------|------|------|--------|-----|-----|-----|-------|-----|-------|-----|-------|-------|--------|-------|-------|------|-------|-----|
| Arch.           | mAP | aero | bike | bird | boat | bottle | bus | car | cat | chair | cow | table | dog | horse | mbike | person | plant | sheep | sofa | train | tv  |
| <b>TY:V1-S</b>  | 23% | 59%  | 10%  | 0%   | 0%   | 0%     | 47% | 52% | 56% | 16%   | 0%  | 0%    | 38% | 7%    | 33%   | 55%    | 0%    | 21%   | 0%   | 47%   | 11% |
| <b>TY:V13-S</b> | 32% | 36%  | 4%   | 22%  | 20%  | 5%     | 54% | 46% | 48% | 9%    | 29% | 34%   | 39% | 45%   | 40%   | 33%    | 5%    | 26%   | 37%  | 45%   | 27% |
| <b>TY:V5-S</b>  | 35% | 39%  | 42%  | 23%  | 22%  | 12%    | 55% | 50% | 42% | 18%   | 31% | 39%   | 35% | 44%   | 4%    | 40%    | 10%   | 33%   | 36%  | 44%   | 32% |
| <b>TY:V8-S</b>  | 39% | 43%  | 48%  | 3%   | 26%  | 15%    | 59% | 51% | 49% | 20%   | 34% | 45%   | 41% | 49%   | 47%   | 42%    | 12%   | 38%   | 41%  | 48%   | 37% |
| <b>TY:V13-B</b> | 40% | 43%  | 49%  | 31%  | 23%  | 11%    | 63% | 52% | 55% | 19%   | 37% | 43%   | 49% | 55%   | 46%   | 39%    | 13%   | 35%   | 47%  | 56%   | 38% |
| <b>TY:V5-B</b>  | 42% | 44%  | 52%  | 30%  | 26%  | 19%    | 61% | 54% | 49% | 24%   | 40% | 46%   | 42% | 52%   | 49%   | 49%    | 18%   | 40%   | 47%  | 51%   | 44% |
| <b>TY:V8-B</b>  | 42% | 43%  | 50%  | 30%  | 27%  | 18%    | 61% | 54% | 50% | 22%   | 44% | 46%   | 46% | 54%   | 49%   | 44%    | 16%   | 40%   | 46%  | 50%   | 42% |

TABLE IV

**QUALITATIVE RESULTS:** TINYISSIMO-V8 RUNNING ON IMAGES CAPTURED WITH OUR SYSTEM (ROW 1) AND WITH IMAGES TAKEN USING AN SLR CAMERA(ROW 2). FOR ALL IMAGES, THE MINIMAL BOUNDING BOX CONFIDENCE SCORE IS 0.25 AND THE MAXIMUM NUMBER OF BOUNDING BOXES PREDICTED IS FIVE.



Optima curve for running the networks quantized on the SoC of GAP9. Fig. 8 shows the TinyissimoYOLOv1.3, v5 and v8 being deployed in both 'small' and 'big' versions. It shows that, while v1.3-Small has the lowest detection robustness, as seen in Table III, it benefits from the lowest inference latency and having the lowest energy consumption. Additionally, the frequency sweep for all the TinyissimoYOLO versions proposed can be used as a look-up table for finding the ideal network's execution frequency. Depending if the application allows for low energy consumption and low accuracy, running TinyissimoYOLOv1.3-small at 150MHz would be the ideal choice or if the application needs fastest inference time and most accuracy, running TinyissimoYOLOv8-Big at 370MHz is the ideal choice.

#### D. Hardware Performance Comparison

We evaluate the performance of TinyissimoYOLOv8-B on three different edge vision hardware platforms: Sony IMX500

<sup>9</sup>, Coral Micro<sup>10</sup>, and GAP9.

As observed from the results, in Table 9, the Sony IMX500 demonstrates the lowest end-to-end latency of 23.88ms, indicating its suitability for real-time applications. However, it has a relatively higher energy consumption of 6.07 mJ compared to GAP9. GAP9, on the other hand, exhibits the lowest energy consumption of 3.54 mJ, making it the most energy-efficient option. Coral Micro falls in between, with a relatively higher latency and energy consumption compared to both Sony IMX500 and GAP9.

The MAC/cycle metric is highest for Sony IMX500 (19.8), followed by GAP9 (14.5), and Coral Micro (10.7). This suggests that Sony IMX500 performs more computations per clock cycle, potentially indicating higher processing power.

In terms of power efficiency, Sony IMX500 and GAP9 have similar power efficiency values of 274.58  $\mu$ W/MHz and 169.32  $\mu$ W/MHz, respectively. Coral Micro, however, has

<sup>9</sup><https://developer.sony.com/imx500/>

<sup>10</sup><https://coral.ai/docs/dev-board-micro/datasheet/>

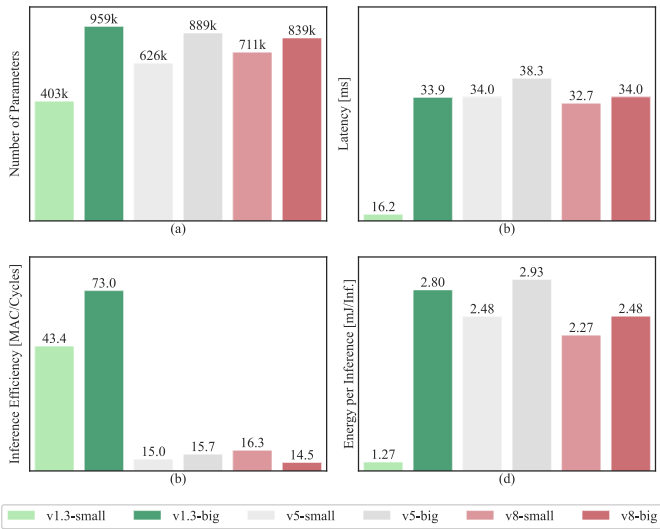


Figure 7. **Deployed TinyissimoYOLO Versions (@0.8V; 370MHz):** This comparison shows a) the number of parameters of each TinyissimoYOLO version b) the latency of each network, c) the inference efficiency, or energy consumption per inference and d) the MAC/cycle, or parallelization workload.

significantly higher power consumption with a value of 5553.2  $\mu\text{W}/\text{MHz}$ .

### E. Battery runtime estimation

The smart glasses are charged with a battery, inserted inside a temple of the smart-glasses, see Fig. 1, with a maximal energy content of up to 154mAh and 585 Wh with a nominal voltage level of around 3.8 V. The continuous execution of the presented system demonstration—the execution of the demonstrator loop—consumes 30.0 mA at 1.8 V continuously and drawing 54 mW from the battery. Further, the HM0360 image sensor consumes 3.2mA during continuous QVGA operation, therefore adding another 5.2mW. Since for the image sensor additional DC-DC converters are needed which operate at 90% efficiency, while the efficiency of the used

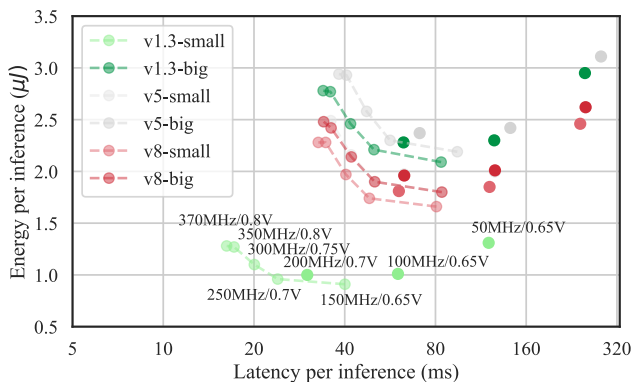


Figure 8. **Latency vs. Energy:** TinyissimoYOLOv1.3, v5 and v8 quantized deployed on GAP9’s NE16 running at different voltage levels and different clocking frequencies.

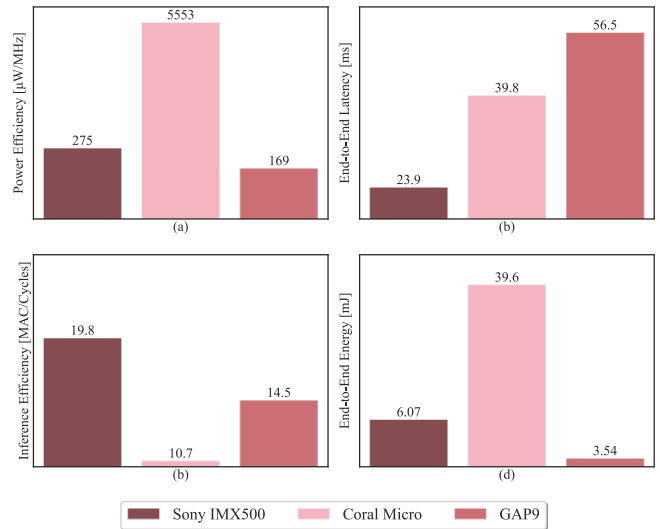


Figure 9. **Performance Evaluation of TinyissimoYOLOv8-Big on Different Hardware Platforms.** Comparison of key metrics, including end-to-end latency, energy consumption, MAC/Cycle ratio, power efficiency, and model parameters, on Sony IMX500, Coral Micro, and GAP9 platforms.

Power Management Integrate Circuit (PMIC) of 95%, the effective power consumption of the image sensor is 6.1 mW. Further, the effective system power draw is 56.8 mW for the loop, while including the camera and the nRF microcontroller leads to 62.9 mW, resulting in a battery runtime of 9.3 h. In perspective the newly released RayBan-Meta smart glasses, with the same sized battery capacity, claim to last 4 hours with moderate usage or up to 3 hours of continuous audio streaming and voice assistance<sup>11</sup>. A system integrating SonyIMX500 instead of GAP9, with an end-to-end power consumption of 254mW, would also discharge the battery in around three and a half hour (at 60 frames per seconds (FPS)).

## VII. LIMITATIONS & FUTURE WORK

While the TinyissimoYOLO network exhibits promising performance, there are certain limitations that warrant consideration. Notably, its reliance on the PascalVOC dataset may lead to challenges in accurately recognizing objects outside the dataset’s scope, see the incorrect prediction of the sofa in the left most figures in row one of Table IV. In future work, extending the network’s training dataset to encompass a broader range of objects, could significantly enhance its applicability. Moreover, the system design might move closer to an AI-In Sensor architecture, similar to Sony IMX500 [10], to further reduce execution time and frame rate and achieve an even more compact form factor. In terms of algorithmic improvement, the next iteration of TinyissimoYOLO might consider Neural Architecture Search, Quantization Aware RepVGG blocks and Knowledge Distillation.

<sup>11</sup><https://www.meta.com/ch/en/legal/ray-ban-meta/disclosures/>

## VIII. CONCLUSION

This paper proposed a novel smart glasses system and demonstrated the system's capabilities using a demonstrator firmware. The demonstrator performs image capturing and demosaicing, before running AI inference. Thereafter, the network's output is post-processed by running a non-max suppression algorithm to get the boundary boxes of the detected networks. The whole demonstrator loop— capture, pre/post process, and running inference— takes 56 ms resulting in about 18fps of continuous demonstrator execution.

Further, this paper proposed a family of new TinyissimoYOLO versions, using the YOLOv3 detection head while evaluating the architectures proposed in TinyissimoYOLOv1, YOLOv5, and YOLOv8. The networks contain 50x to 100x fewer parameters compared to the initial YOLOv1 version and have been evaluated and compared on the PascalVOC test dataset. The best performing big versions of TinyissimoYOLOv5 and v8 with 890 k and 840 k parameters respectively, achieve 42% mAP while being executed within 38.3 ms and 34 ms on the GAP9 microcontrollers NE16 accelerator. The fastest small TinyissimoYOLOv1.3 is executed within 16.2 ms consuming only 1.27 mJ of energy for one inference and achieves 32% mAP. As such, this paper presents a highly generalized multi-class detection family of networks running with SOTA performance detection accuracy in real-time (>16fps) on the GAP9 microcontroller.

## REFERENCES

- [1] D. Nahavandi, R. Alizadehsani, A. Khosravi, and U. R. Acharya, "Application of artificial intelligence in wearable devices: Opportunities and challenges," *Computer Methods and Programs in Biomedicine*, vol. 213, p. 106541, 2022.
- [2] S. Bian, X. Wang, T. Polonelli, and M. Magno, "Exploring automatic gym workouts recognition locally on wearable resource-constrained devices," in *2022 IEEE 13th International Green and Sustainable Computing Conference (IGSC)*. IEEE, 2022, pp. 1–6.
- [3] H. Sun and K. Kim, "Design of glasses products based on artificial intelligence," in *The International Conference on Cyber Security Intelligence and Analytics*. Springer, 2022, pp. 1051–1058.
- [4] C. Spandonidis, F. Giannopoulos, J. Agulló, N. S. Tachos, L. Frederiksen, A. Martín, and R. G. Carvajal, "Development of visual sensors and augmented reality based smart glasses for enhancement of business sustainability and wellbeing of the aging workforce," *IEEE Instrumentation & Measurement Magazine*, vol. 26, no. 6, pp. 21–27, 2023.
- [5] M. Z. Iqbal and A. G. Campbell, "Adopting smart glasses responsibly: potential benefits, ethical, and privacy concerns with ray-ban stories," *AI and Ethics*, vol. 3, no. 1, pp. 325–327, 2023.
- [6] M. R. Miah and M. S. Hussain, "A unique smart eye glass for visually impaired people," in *2018 International Conference on Advancement in Electrical and Electronic Engineering (ICAEEE)*. IEEE, 2018, pp. 1–4.
- [7] E. Ali Hassan and T. B. Tang, "Smart glasses for the visually impaired people," in *Computers Helping People with Special Needs: 15th International Conference, ICCHP 2016, Linz, Austria, July 13-15, 2016, Proceedings, Part II 15*. Springer, 2016, pp. 579–582.
- [8] X. Feng, Y. Jiang, X. Yang, M. Du, and X. Li, "Computer vision algorithms and hardware implementations: A survey," *Integration*, vol. 69, pp. 309–320, 2019.
- [9] X. Wang, M. Magno, L. Cavigelli, M. Mahmud, C. Cecchetto, S. Vasanelli, and L. Benini, "Embedded classification of local field potentials recorded from rat barrel cortex with implanted multi-electrode array," in *2018 IEEE Biomedical Circuits and Systems Conference (BioCAS)*. IEEE, 2018, pp. 1–4.
- [10] P. Bonazzi, T. Ruegg, S. Bian, Y. Li, and M. Magno, "Tinytracker: Ultrafast and ultra-low-power edge vision for in-sensor gaze estimation," *2023 IEEE Sensors Conference*, 2023.
- [11] X. Wang, M. Hersche, M. Magno, and L. Benini, "Mi-bminet: An efficient convolutional neural network for motor imagery brain-machine interfaces with eeg channel selection," *arXiv preprint arXiv:2203.14592*, 2022.
- [12] A. Moin, A. Zhou, A. Rahimi, A. Menon, S. Benatti, G. Alexandrov, S. Tamakloe, J. Ting, N. Yamamoto, Y. Khan *et al.*, "A wearable biosensing system with in-sensor adaptive machine learning for hand gesture recognition," *Nature Electronics*, vol. 4, no. 1, pp. 54–63, 2021.
- [13] W. X. Zhao, K. Zhou, J. Li, T. Tang, X. Wang, Y. Hou, Y. Min, B. Zhang, J. Zhang, Z. Dong *et al.*, "A survey of large language models," *arXiv preprint arXiv:2303.18223*, 2023.
- [14] W. Wang, J. Dai, Z. Chen, Z. Huang, Z. Li, X. Zhu, X. Hu, T. Lu, L. Lu, H. Li, X. Wang, and Y. Qiao, "Internimage: Exploring large-scale vision foundation models with deformable convolutions," in *Proceedings of the IEEE/CVF Conference on Computer Vision and Pattern Recognition (CVPR)*, June 2023, pp. 14 408–14 419.
- [15] J. Huang, G. Huang, Z. Zhu, Y. Ye, and D. Du, "Bevdet: High-performance multi-camera 3d object detection in bird-eye-view," *arXiv preprint arXiv:2112.11790*, 2021.
- [16] Z. Li, W. Wang, H. Li, E. Xie, C. Sima, T. Lu, Y. Qiao, and J. Dai, "Bevformer: Learning bird's-eye-view representation from multi-camera images via spatiotemporal transformers," in *European conference on computer vision*. Springer, 2022, pp. 1–18.
- [17] J. McCormac, R. Clark, M. Bloesch, A. Davison, and S. Leutenegger, "Fusion++: Volumetric object-level slam," in *2018 international conference on 3D vision (3DV)*. IEEE, 2018, pp. 32–41.
- [18] A. Rosinol, M. Abate, Y. Chang, and L. Carlone, "Kimera: an open-source library for real-time metric-semantic localization and mapping," in *2020 IEEE International Conference on Robotics and Automation (ICRA)*. IEEE, 2020, pp. 1689–1696.
- [19] J. Crespo, J. C. Castillo, O. M. Mozos, and R. Barber, "Semantic information for robot navigation: A survey," *Applied Sciences*, vol. 10, no. 2, p. 497, 2020.
- [20] F. Samie, L. Bauer, and J. Henkel, "From cloud down to things: An overview of machine learning in internet of things," *IEEE Internet of Things Journal*, vol. 6, no. 3, pp. 4921–4934, 2019.
- [21] S. S. Saha, S. S. Sandha, and M. Srivastava, "Machine learning for microcontroller-class hardware—a review," *IEEE Sensors Journal*, 2022.
- [22] J. Redmon, S. Divvala, R. Girshick, and A. Farhadi, "You only look once: Unified, real-time object detection," in *Proceedings of the IEEE conference on computer vision and pattern recognition*, 2016, pp. 779–788.
- [23] P. Jiang, D. Ergu, F. Liu, Y. Cai, and B. Ma, "A review of yolo algorithm developments," *Procedia Computer Science*, vol. 199, pp. 1066–1073, 2022.
- [24] G. Premsankar, M. Di Francesco, and T. Taleb, "Edge computing for the internet of things: A case study," *IEEE Internet of Things Journal*, vol. 5, no. 2, pp. 1275–1284, 2018.
- [25] F. Conti, G. Paulin, D. Rossi, A. Di Mauro, G. Rutishauser, G. Ottavi, M. Eggimann, H. Okuhara, and L. Benini, "Marsellus: A heterogeneous risc-v ai-iot end-node soc with 2-to-8b dnn acceleration and 30%-boost adaptive body biasing," *arXiv preprint arXiv:2305.08415*, 2023.
- [26] G. Islamoglu, M. Scherer, G. Paulin, T. Fischer, V. J. Jung, A. Garofalo, and L. Benini, "Ita: An energy-efficient attention and softmax accelerator for quantized transformers," in *2023 IEEE/ACM International Symposium on Low Power Electronics and Design (ISLPED)*. IEEE, 2023, pp. 1–6.
- [27] A. Reuther, P. Michaleas, M. Jones, V. Gadepally, S. Samsi, and J. Kepner, "Survey of machine learning accelerators," in *2020 IEEE High Performance Extreme Computing Conference (HPEC)*, 2020, pp. 1–12.
- [28] J. Moosmann, M. Giordano, C. Vogt, and M. Magno, "Tinyssimoyolo: A quantized, low-memory footprint, tinyml object detection network for low power microcontrollers," *arXiv preprint arXiv:2306.00001*, 2023.
- [29] J. Redmon and A. Farhadi, "Yolo9000: better, faster, stronger," in *Proceedings of the IEEE conference on computer vision and pattern recognition*, 2017, pp. 7263–7271.
- [30] —, "Yolov3: An incremental improvement," *arXiv preprint arXiv:1804.02767*, 2018.
- [31] A. Bochkovskiy, C.-Y. Wang, and H.-Y. M. Liao, "Yolov4: Optimal speed and accuracy of object detection," *arXiv preprint arXiv:2004.10934*, 2020.

- [32] C. Li, L. Li, H. Jiang, K. Weng, Y. Geng, L. Li, Z. Ke, Q. Li, M. Cheng, W. Nie *et al.*, “Yolov6: A single-stage object detection framework for industrial applications,” *arXiv preprint arXiv:2209.02976*, 2022.
- [33] C.-Y. Wang, A. Bochkovskiy, and H.-Y. M. Liao, “Yolov7: Trainable bag-of-freebies sets new state-of-the-art for real-time object detectors,” in *Proceedings of the IEEE/CVF Conference on Computer Vision and Pattern Recognition*, 2023, pp. 7464–7475.
- [34] G. Jocher, A. Chaurasia, and J. Qiu, “YOLO by Ultralytics,” Jan. 2023. [Online]. Available: <https://github.com/ultralytics/ultralytics>
- [35] G. Jocher, “YOLOv5 by Ultralytics,” May 2020. [Online]. Available: <https://github.com/ultralytics/yolov5>
- [36] M. Liang and X. Hu, “Recurrent convolutional neural network for object recognition,” in *2015 IEEE Conference on Computer Vision and Pattern Recognition (CVPR)*, 2015, pp. 3367–3375.
- [37] R. Girshick, “Fast r-cnn,” in *Proceedings of the IEEE international conference on computer vision*, 2015, pp. 1440–1448.
- [38] K. He, G. Gkioxari, P. Dollár, and R. Girshick, “Mask r-cnn,” in *Proceedings of the IEEE international conference on computer vision*, 2017, pp. 2961–2969.
- [39] W. Liu, D. Anguelov, D. Erhan, C. Szegedy, S. Reed, C.-Y. Fu, and A. C. Berg, “Ssd: Single shot multibox detector,” in *Computer Vision—ECCV 2016: 14th European Conference, Amsterdam, The Netherlands, October 11–14, 2016, Proceedings, Part I 14*. Springer, 2016, pp. 21–37.
- [40] C.-Y. Fu, W. Liu, A. Ranga, A. Tyagi, and A. C. Berg, “Dssd: Deconvolutional single shot detector,” *arXiv preprint arXiv:1701.06659*, 2017.
- [41] H.-T. Pham, M.-A. Nguyen, and C.-C. Sun, “Aiot solution survey and comparison in machine learning on low-cost microcontroller,” in *2019 International Symposium on Intelligent Signal Processing and Communication Systems (ISPACS)*, 2019, pp. 1–2.
- [42] V. Kamath and A. Renuka, “Deep learning based object detection for resource constrained devices-systematic review, future trends and challenges ahead,” *Neurocomputing*, 2023.
- [43] K. Han, Y. Wang, H. Chen, X. Chen, J. Guo, Z. Liu, Y. Tang, A. Xiao, C. Xu, Y. Xu *et al.*, “A survey on vision transformer,” *IEEE transactions on pattern analysis and machine intelligence*, vol. 45, no. 1, pp. 87–110, 2022.
- [44] Y. Li, K. Zhang, J. Cao, R. Timofte, and L. Van Gool, “Localvit: Bringing locality to vision transformers,” *arXiv preprint arXiv:2104.05707*, 2021.
- [45] A. A. Süzen, B. Duman, and B. Şen, “Benchmark analysis of jetson tx2, jetson nano and raspberry pi using deep-cnn,” in *2020 International Congress on Human-Computer Interaction, Optimization and Robotic Applications (HORA)*. IEEE, 2020, pp. 1–5.
- [46] P. S. Mittapalli, M. Tagore, P. A. Reddy, G. B. Kande, and Y. M. Reddy, “Deep learning based real-time object detection on jetson nano embedded gpu,” in *Microelectronics, Circuits and Systems: Select Proceedings of Micro2021*. Springer, 2023, pp. 511–521.
- [47] T. Liang, J. Glossner, L. Wang, S. Shi, and X. Zhang, “Pruning and quantization for deep neural network acceleration: A survey,” *Neurocomputing*, vol. 461, pp. 370–403, 2021.
- [48] S. Bianco, R. Cadene, L. Celona, and P. Napoletano, “Benchmark analysis of representative deep neural network architectures,” *IEEE access*, vol. 6, pp. 64270–64277, 2018.
- [49] J. Gou, B. Yu, S. J. Maybank, and D. Tao, “Knowledge distillation: A survey,” *International Journal of Computer Vision*, vol. 129, pp. 1789–1819, 2021.
- [50] J. Moosmann, H. Mueller, N. Zimmerman, G. Rutishauser, L. Benini, and M. Magno, “Flexible and fully quantized ultra-lightweight tinyssimoyolo for ultra-low-power edge systems,” *arXiv preprint arXiv:2307.05999*, 2023.
- [51] M. Scherer, F. Sidler, M. Rogenmoser, M. Magno, and L. Benini, “Widevision: A low-power, multi-protocol wireless vision platform for distributed surveillance,” in *2022 18th International Conference on Wireless and Mobile Computing, Networking and Communications (WiMob)*. IEEE, 2022, pp. 394–399.
- [52] T. Ruegg, P. Bonazzi, and A. Ronco, “Gaze estimation on spresense,” 2023.
- [53] G. Rutishauser, M. Scherer, T. Fischer, and L. Benini, “7  $\mu$ j/inference end-to-end gesture recognition from dynamic vision sensor data using ternarized hybrid convolutional neural networks,” *Future Generation Computer Systems*, vol. 149, pp. 717–731, 2023.
- [54] E. Liberis, Ł. Dudziak, and N. D. Lane, “ $\mu$ nas: Constrained neural architecture search for microcontrollers,” in *Proceedings of the 1st Workshop on Machine Learning and Systems*, 2021, pp. 70–79.
- [55] I. Fedorov, R. P. Adams, M. Mattina, and P. Whatmough, “Sparse architecture search for cnns on resource-constrained microcontrollers,” *Advances in Neural Information Processing Systems*, vol. 32, 2019.
- [56] S. Han, H. Mao, and W. J. Dally, “Deep compression: Compressing deep neural networks with pruning, trained quantization and Huffman coding,” *arXiv preprint arXiv:1510.00149*, 2015.
- [57] G. Rutishauser, F. Conti, and L. Benini, “Free bits: Latency optimization of mixed-precision quantized neural networks on the edge,” in *2023 IEEE 5th International Conference on Artificial Intelligence Circuits and Systems (AICAS)*. IEEE, 2023, pp. 1–5.
- [58] I. Hubara, M. Courbariaux, D. Soudry, R. El-Yaniv, and Y. Bengio, “Quantized neural networks: Training neural networks with low precision weights and activations,” *The Journal of Machine Learning Research*, vol. 18, no. 1, pp. 6869–6898, 2017.
- [59] A. Nadalini, G. Rutishauser, A. Burrello, N. Bruschi, A. Garofalo, L. Benini, F. Conti, and D. Rossi, “A 3 tops/w risc-v parallel cluster for inference of fine-grain mixed-precision quantized neural networks,” in *2023 IEEE Computer Society Annual Symposium on VLSI (ISVLSI)*. IEEE, 2023, pp. 1–6.
- [60] Y. Li, S. Gu, C. Mayer, L. V. Gool, and R. Timofte, “Group sparsity: The hinge between filter pruning and decomposition for network compression,” in *Proceedings of the IEEE/CVF conference on computer vision and pattern recognition*, 2020, pp. 8018–8027.
- [61] F. Zhou and Y. Chai, “Near-sensor and in-sensor computing,” *Nature Electronics*, vol. 3, no. 11, pp. 664–671, 2020.
- [62] S. Angizi, S. Tabrizchi, and A. Roohi, “Pisa: A binary-weight processing-in-sensor accelerator for edge image processing,” *arXiv preprint arXiv:2202.09035*, 2022.
- [63] P. Warden and D. Situnayake, *Tinyml: Machine learning with tensorflow lite on arduino and ultra-low-power microcontrollers*. O’Reilly Media, 2019.
- [64] L. Lai, N. Suda, and V. Chandra, “Cmsis-nn: Efficient neural network kernels for arm cortex-m cpus,” *arXiv preprint arXiv:1801.06601*, 2018.
- [65] C. Liu, S. Chen, T.-H. Tsai, B. De Salvo, and J. Gomez, “Augmented reality—the next frontier of image sensors and compute systems,” in *2022 IEEE International Solid-State Circuits Conference (ISSCC)*, vol. 65. IEEE, 2022, pp. 426–428.
- [66] L.-H. Lee and P. Hui, “Interaction methods for smart glasses: A survey,” *IEEE Access*, vol. 6, pp. 28712–28732, 2018.
- [67] I. Hong, K. Bong, D. Shin, S. Park, K. J. Lee, Y. Kim, and H.-J. Yoo, “A 2.71 nj/pixel gaze-activated object recognition system for low-power mobile smart glasses,” *IEEE Journal of Solid-State Circuits*, vol. 51, no. 1, pp. 45–55, 2015.
- [68] M. Salvaro, S. Benatti, V. Kartsch, M. Guermendi, and L. Benini, “A wearable device for brain-machine interaction with augmented reality head-mounted display,” in *EAI International Conference on Body Area Networks*. Springer, 2018, pp. 339–351.
- [69] W.-J. Chang, L.-B. Chen, C.-H. Hsu, J.-H. Chen, T.-C. Yang, and C.-P. Lin, “Medglasses: A wearable smart-glasses-based drug pill recognition system using deep learning for visually impaired chronic patients,” *IEEE Access*, vol. 8, pp. 17013–17024, 2020.
- [70] F. Subhan, A. Mirza, M. B. M. Su’ud, M. M. Alam, S. Nisar, U. Habib, and M. Z. Iqbal, “Ai-enabled wearable medical internet of things in healthcare system: A survey,” *Applied Sciences*, vol. 13, no. 3, p. 1394, 2023.
- [71] O. Danielsson, M. Holm, and A. Syberfeldt, “Augmented reality smart glasses for operators in production: Survey of relevant categories for supporting operators,” *Procedia CIRP*, vol. 93, pp. 1298–1303, 2020.
- [72] P. Schilk, N. Polvani, A. Ronco, M. Cernak, and M. Magno, “In-ear-voice: Towards milli-watt audio enhancement with bone-conduction microphones for in-ear sensing platforms,” in *Proceedings of the 8th ACM/IEEE Conference on Internet of Things Design and Implementation*, 2023, pp. 1–12.
- [73] M. Everingham, L. Van Gool, C. K. Williams, J. Winn, and A. Zisserman, “The pascal visual object classes (voc) challenge,” *International journal of computer vision*, vol. 88, pp. 303–338, 2010.
- [74] M. Giordano, L. Piccinelli, and M. Magno, “Survey and comparison of milliwatts micro controllers for tiny machine learning at the edge,” in *2022 IEEE 4th International Conference on Artificial Intelligence Circuits and Systems (AICAS)*. IEEE, 2022, pp. 94–97.